Antitumor and Antimetastatic Activity of IL-23[1]

Chia-Hui Lo,*† Shan-Chih Lee,[2]* Pin-Yi Wu,* Wen-Yu Pan,*† Jui Su,* Chao-Wen Cheng,§ Steve R. Roffler,* Bor-Luen Chiang,‡ Chun-Nan Lee,† Cheng-Wen Wu,¶ and Mi-Hua Tao[3]*

The structure and T cell stimulatory effects of the recently discovered cytokine IL-23 are similar to, but distinct from, those of IL-12. Although the antitumor activities of IL-12 are well characterized, the effect of IL-23 on tumor growth is not known. In this study, murine CT26 colon adenocarcinoma and B16F1 melanoma cells were engineered using retroviral vectors to release single-chain IL-23 (scIL-23) to evaluate its antitumor activity. In BALB/c mice, scIL-23-transduced CT26 cells grew progressively until day 26 to an average size of 521 ± 333 mm^3, then the tumors started to regress in most animals, resulting in a final 70% rate of complete tumor rejection. scIL-23 transduction also significantly suppressed lung metastases of CT26 and B16F1 tumor cells. In addition, mice that rejected scIL-23-transduced tumors developed a memory response against subsequent wild-type tumor challenge. Compared with scIL-12-expressing CT26 cells, scIL-23-transduced tumors lacked the early response, but achieved comparable antitumor and antimetastatic activity. These results demonstrated that IL-23, like IL-12, provided effective protection against malignant diseases, but it probably acted by different antitumor mechanisms. As a first step in identifying these antitumor mechanisms, tumor challenge studies were performed in immunocompromised hosts and in animals selectively depleted of various lymphocyte populations. The results showed that CD8$^+$ T cells, but not CD4$^+$ T cells or NK cells, were crucial for the antitumor activity of IL-23. ***The Journal of Immunology*****, 2003, 171: 600–607.**

The recently discovered cytokine IL-23 consists of a heterodimer of the IL-12 p40 subunit and a novel 19-kDa protein, termed p19 (1). Structurally, p19 is distantly related to IL-6, G-CSF, and the IL-12 p35 subunit (1). Although p19 is expressed in various tissues and cell types, per se it lacks biological activity (1) and only becomes biologically active when complexed with p40, which is normally secreted by activated macrophages and dendritic cells. IL-23 preferentially induces proliferation of, and IFN-γ production by, memory T cells as opposed to naive T cells, whereas the effects of IL-12 are mainly restricted to naive T cells (1). The receptor for IL-23 is composed of the IL-12R β1 subunit and a novel IL-23R subunit (2). The differential response of naive and memory T cells to IL-12 and IL-23 correlates well with the preferential expression of the IL-12R β2 subunit on naive T cells and of the IL-23R subunit on memory T cells (2).

IL-12 has potent antitumor activity in a variety of murine tumor models, causing regression of established tumors (3–5) and inhibiting the formation of experimental metastases (3, 4) and spontaneous metastases (6, 7). Whether IL-23 possesses antitumor activity is unknown. In this study, we used a retroviral vector to engineer a murine colon adenocarcinoma cell line, CT26, to produce a single-chain IL-23 (scIL-23),[4] and we demonstrated that local production of IL-23 inhibits s.c. and metastatic tumor growth in vivo. The antitumor activity of IL-23 requires CD8$^+$ T cells, but not CD4$^+$ T cells or NK cells. This is, as far as we are aware, the first report showing that IL-23 possesses potent antitumor activity.

Materials and Methods

Mice

Female BALB/c and C57BL/6 mice were purchased from the National Laboratory Animal Breeding and Research Center (Taipei, Taiwan). Female SCID (C.B17 *scid/scid*) and SCID-beige (C.B17 *scid/beige*) mice were purchased from the Laboratory Animal Center, National Taiwan University College of Medicine (Taipei, Taiwan). All animal experiments were conducted in specific pathogen-free conditions and in accordance with the guidelines approved by the Animal Care and Usage Committee of the Institute of Biomedical Sciences (Academia Sinica, Taipei, Taiwan).

Cells and depletion Abs

CT26 is a colon adenocarcinoma cell line derived from BALB/c mice treated with *N*-nitroso-*N*-methylurethane (8). B16F1 is a metastasizing subline of the B16 melanoma that arose spontaneously and is syngeneic with C57BL/6 mice (9). 3T3 (CCL-163; American Type Culture Collection, Manassas, VA) is a murine fibroblast cell line derived from BALB/c mice. Cell lines were maintained in DMEM, 10% heat-inactivated FCS, 2 mM L-glutamine, 100 U/ml penicillin, and 100 μg/ml streptomycin at 37°C in a 5% CO_2 humidified incubator. Anti-CD4 (GK1.5, rat IgG2b) and anti-CD8 (53-6.72, rat IgG2a) hybridomas, purchased from the American Type Culture Collection, were injected into pristine-treated SCID mice to generate ascites and the IgG purified by protein G Sepharose chromatography (Amersham Pharmacia, New Territories, Hong Kong). Normal rat IgG was similarly produced from a hybridoma clone (HAA, rat IgG2a) derived from a naive Sprague-Dawley rat. Rabbit anti-asialo GM1 antiserum was purchased from Wako Pure Chemical (Osaka, Japan). Normal rabbit serum was purchased from Biowest (Nuailles, France).

Vector construction and retroviral infection

cDNA encoding murine p19 was obtained by reverse transcription and PCR amplification of RNA derived from the mouse macrophage cell line A3.1A7 (kindly provided by K. L. Rock, Dana-Farber Cancer Institute, Boston MA). To facilitate gene cloning into retroviral vectors, an overlap

*Institute of Biomedical Sciences, Academia Sinica, Taipei, Taiwan; †Graduate Institute of Medical Technology and ‡Graduate Institute of Clinical Medicine, National Taiwan University, Taipei, Taiwan; §Graduate Institute of Life Sciences, National Defense Medical Center, Taipei, Taiwan; and ¶National Health Research Institutes, Taipei, Taiwan

Received for publication March 12, 2003. Accepted for publication May 15, 2003.

The costs of publication of this article were defrayed in part by the payment of page charges. This article must therefore be hereby marked *advertisement* in accordance with 18 U.S.C. Section 1734 solely to indicate this fact.

[1] This work was supported by Grant NSC-91-3112-P-001-026-Y from the National Science Council and Grant NHRI-CN-PL-9101P from the National Health Research Institutes (Taipei, Taiwan).

[2] Current address: Institute of Bioinformatics, Taichung Healthcare and Management University, Taichung, Taiwan 413.

[3] Address correspondence and reprint requests to Dr. Mi-Hua Tao, 128 Yen-Chiu-Yuan Road, Section 2, Institute of Biomedical Sciences, Academia Sinica, Taipei, Taiwan 115. E-mail address: bmtao@ibms.sinica.edu.tw

[4] Abbreviation used in this paper: sc, single chain.

0022-1767/03/$02.00

PCR strategy (10) was used to generate an scIL-23 cDNA in the p40-p19 orientation. Briefly, the p19 fragment was PCR amplified with the signal sequence replaced with a sequence encoding the GSTSGSGKPGSGEG STKG peptide linker. The forward primer was 5′-GAGGGTAGTACTA AGGGTCTGGCTGTGCCTAGGAGTAGC-3′ and the reverse primer was 5′-GGGGTTTAAGCTGTTGCCACTAAGGGCTCAGTCAG-3′. The IL-12 p40 fragment was PCR amplified as described previously (10). The p19 and p40 fragments were then used as templates in a second-round PCR, and the final amplified product containing the p40-linker-p19 sequence was ligated into pCR-Blunt (Invitrogen, Carlsbad, CA) for sequencing and subsequent cloning. The pBlunt plasmid was digested at the *Xho*I and *Hin*dIII sites to release the DNA fragment, which was then inserted into the pLNCX2 retroviral vector (BD Clontech, Palo Alto, CA) to produce the plasmid pLNCX/scIL-23 (Fig. 1*A*). The *Sal*I-*Bam*HI fragment from the plasmid pscIL-12.2 (10), which encodes a functional scIL-12 protein, was inserted into the *Xho*I-*Bam*HI sites in pLNCX2 to produce the plasmid pLNCX/scIL-12 (Fig. 1*A*).

Retroviral supernatant was generated by transfecting pLNCX/scIL-23 or pLNCX/scIL-12 proviral constructs into the PT67 packaging cell line (BD Clontech) using lipofectamine 2000 (Life Technologies, Grand Island, NY). CT26 cells (2×10^4 cells/well in six-well plates) were infected for 24 h with 2.5 ml of scIL-23 or scIL-12 retroviral supernatant in the presence of 4 μg/ml polybrene. After washing, the cells were incubated for 48 h in DMEM/10% FCS medium and then were selected in 0.5 mg/ml G418 and screened for secretion of IL-23 or IL-12 (CT26/scIL-23 and CT26/scIL-12, respectively). G418-resistant CT26 cells infected with the pLNCX2 vector alone (CT26/LNCX) were used as controls. B16F1 cells were similarly infected with scIL-23 or the control LNCX2 retroviral supernatant and were selected in 1.2 mg/ml G418 to produce B16F1/scIL-23 and B16F1/LNCX cells, respectively.

Expression of single-chain cytokine proteins

3T3 cells (1×10^6) were transiently transfected with 5 μg of pLNCX/scIL-23, pLNCX/scIL-12, or the empty vector pLNCX2 using lipofectamine 2000. After 24-h incubation, the supernatants were harvested for functional analysis and the cells were metabolically labeled for an additional 18 h with 150 μCi/ml Pro-mix L-[^{35}S] in vitro cell-labeling mix (Amersham Pharmacia) in cysteine/methionine-free DMEM (Sigma-Aldrich, St. Louis, MO). Proteins were immunoprecipitated by addition of 3 μg of rat anti-mouse IL-12 p40/p70 mAb (C17.8; BD PharMingen, San Diego, CA) followed by protein G Sepharose. The precipitates were electrophoresed on SDS polyacrylamide gels and visualized by autoradiography on Kodak-MR film (Kodak, Rochester, NY).

Biofunctional assay of single-chain cytokine proteins

For the cytokine functional assay, CD4$^+$ T cells from the spleen and lymph nodes of naive mice were enriched using nylon wool followed by selection with a magnetically labeled anti-CD4 mAb (L3T4; Miltenyi Biotec, Auburn, CA) using the MACS system (Miltenyi Biotec). FACS analysis of the purified CD4$^+$ T cells showed >95% purity (data not shown). The purified CD4$^+$ T cells (2×10^4/well) were then cultured for 5 days in wells coated with anti-CD3 mAb 145.2C11 (CRL-1975; American Type Culture Collection) in medium containing serial dilutions of test samples. To measure IFN-γ release, the cell-free supernatants were prepared and assayed using a sandwich ELISA, with the capture mAb being R4-6A2 (rat IgG1; BD PharMingen) and the detection biotinylated mAb being XMG1.2 (rat IgG1; BD PharMingen). The ELISA was performed according to the manufacturer's instructions and has been described previously (11). To measure proliferation, the cells were pulsed for 18 h with [^{3}H]thymidine (1 μCi per well) and the incorporated radioactivity was determined as described previously (11).

Tumor growth and metastasis

Exponentially growing tumor cells were harvested and used to induce s.c. tumors or metastases only if their viability exceeded 95%, as determined by trypan blue staining. To measure the tumorigenicity of control (CT26 cells or CT26/LNCX cells) and scIL-12- or scIL-23-transduced CT26 cells, groups of BALB/c mice ($n = 10$) were injected s.c. with 1×10^5 cells of each tumor cell line in 100 μl of Dulbecco's PBS (Sigma-Aldrich). Tumor growth was measured two to three times per week, and the mean volume in cubic millimeters and the SD for each group were calculated as described previously (12). The mice were killed when the tumor reached >3000 mm^3. In some experiments, mice that had rejected the tumors were rechallenged s.c. with 1×10^5 nontransduced CT26 cells in the other flank on day 60 after the initial tumor implantation to evaluate induction of antitumor immunity.

Immune-deficient mice and mice deleted selectively of certain lymphocyte populations by in vivo Ab treatment were used to evaluate the relative contribution of various immune cells to IL-23-mediated antitumor activity. Groups of SCID (deficient in T cells and B cells) and SCID/beige mice (deficient in T cells, B cells, and NK cells) were injected s.c. with 1×10^5 CT26/scIL-23 or control CT26/LNCX cells. For in vivo Ab depletion experiments, BALB/c mice were injected s.c. with 1×10^5 CT26/scIL-23 cells on day 0. CD4$^+$ and CD8$^+$ T cells were depleted by i.p. injection of 0.5 mg of anti-CD4 mAb (GK1.5) and anti-CD8 mAb (53-6.72), respectively, on day -2, and then with 0.25 mg of the same mAb on days 0, 3, 5, 12, 19, 26, 33, 40, and 47. NK cells were depleted by i.p. injection of 20 μl of rabbit anti-asialo GM1 antiserum using the same schedule. Mice injected i.p. with normal rat IgG or normal rabbit serum at the same dose and schedule were used as controls. Tumor growth and the number of survivors in each group were monitored as described above.

In the lung metastasis model, BALB/c mice were given 2×10^5 CT26/LNCX, CT26/scIL-23, or CT26/scIL-12 cells, and C57BL/6 mice were given 2×10^5 B16F1/LNCX or B16F1/scIL-23 cells in 0.1 ml of PBS by tail vein injection. Experimental metastases were evaluated 21 days after tumor inoculation. The tumor nodules were contrasted using black india ink before counting under a dissecting microscope.

Cytotoxicity assays

Spleen cells (2×10^6 per well) from mice that were tumor free at 60 days after initial tumor injection or from age-matched naive mice were incubated for 5 days with mitomycin C-treated CT26 cells (5×10^5 per well) in the presence of 5 U/ml recombinant human IL-2 in 24-well plates. Target cells (CT26 cells or peptide-pulsed P815 cells) were radiolabeled with chromium-51 (Amersham Pharmacia). The H2-L^d-restricted AH1 peptide (SPSYVYHQF) (13) and the QL9 peptide (QLSPFPFDL) (14) were purchased from Kelowna (Taipei, Taiwan) and used at 40 μg/ml to pulse cells. The previously described chromium release assay was used to measure the ability of in vitro-stimulated responder cells to lyse target cells (11).

Immunohistochemistry

Tumor specimens were fixed in periodate-lysine-paraformaldehyde for 3 h and then were transferred to 20% sucrose for 3–4 h. The fixed tissues were

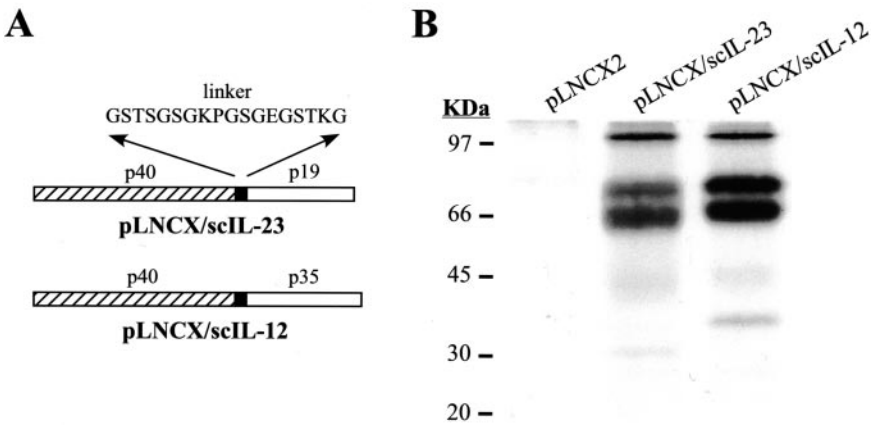

FIGURE 1. Construction and expression of scIL-23. *A*, Schematic diagram of pLNCX/scIL-23 and pLNCX/scIL-12. The single-chain proteins scIL-23 and scIL-12 were in the p40-p19 and p40-p35 orientation, separated by a flexible 18-aa peptide linker. *B*, 3T3 fibroblasts were transiently transfected with the proviral plasmids for 24 h, and then were metabolically labeled with Pro-mix L-[^{35}S] for an additional 18 h. Proteins in the supernatant were immunoprecipitated using an anti-p40 mAb and were analyzed on an SDS polyacrylamide gel.

embedded in OCT compound (Sakura Finetek, Torrance, CA), snap frozen in liquid nitrogen, and stored at −80°C. Cryostat cut sections (5 μm) were fixed in cold acetone and blocked with 2% BSA for 30 min. After two washes in Tris buffer, the slides were incubated overnight at 4°C with biotinylated rat mAbs (1/100) directed against mouse CD4 (CT-CD4; Serotec, Oxford, U.K.) or CD8 (KT-15; Immunotech, Marseille, France). Isotype-matched biotinylated rat IgGs were used as negative controls. Endogenous peroxidase activity was quenched with 0.6% (v/v) H_2O_2 in methanol, then streptavidin peroxidase (DAKO, Carpinteria, Denmark) and 3,3′-diaminobenzidine substrate-chromogen solution (DAKO) were added. After a thorough wash in distilled water, the slides were counterstained with hematoxylin and analyzed by light microscopy at ×200 magnification.

Statistics

The statistical significance of differences between experimental groups of animals was determined using Student's *t* test. Findings were regarded as significant if the two-tailed *p* value was ≤0.05.

Results

Construction and expression of the retroviral vector encoding scIL-23

The scIL-12 and scIL-23 gene fragments were constructed as described in *Materials and Methods* and subcloned into the retroviral vector pLNCX2. The resulting proviral constructs, pLNCX/scIL-12 and pLNCX/scIL-23, encode, respectively, the p40-linker-p35 and p40-linker-p19 fusion proteins (Fig. 1*A*). 3T3 cells were transiently transfected with pLNCX/scIL-12, pLNCX/scIL-23, or the parental pLNCX2 plasmid, and the protein products in the supernatant were analyzed by immunoprecipitation with p40-specific mAb. Plasmid pLNCX/scIL-23 generated two proteins of 73 and 69 kDa, whereas pLNCX/scIL-12 gave two proteins of 75 and 71 kDa (Fig. 1*B*). The double bands in both cases are probably due to glycosylation (1, 15). The control vector did not produce proteins recognized by the anti-p40 mAb.

To investigate the functional activities of the fusion cytokines, the conditioned medium from pLNCX2-, pLNCX/scIL-12-, or pLNCX/scIL-23-transfected 3T3 fibroblasts was tested for its ability to stimulate purified $CD4^+$ T cells in the presence of plate-bound anti-CD3 mAb. As shown in Fig. 2*A*, the scIL-23-containing supernatant stimulated the proliferation of $CD4^+$ T cells in a dose-dependent manner and to the same degree as the scIL-12-containing supernatant. In contrast, the scIL-23-containing supernatant failed to induce IFN-γ production, whereas the scIL-12-containing supernatant strongly stimulated IFN-γ secretion (Fig. 2*B*). The pLNCX2 plasmid failed to stimulate the proliferation of $CD4^+$ T cells and IFN-γ secretion.

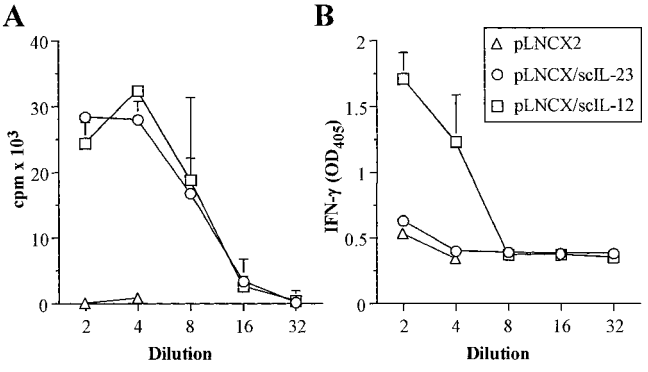

FIGURE 2. Functional assay of scIL-23. 3T3 cells were transfected with various proviral plasmids for 48 h, and then the culture supernatants were collected for the functional assay. Purified mouse $CD4^+$ T cells were cultured for 5 days with serial dilutions of transfected cell culture supernatants in the presence of plate-bound anti-CD3 mAb, and then cell proliferation was assessed by [^{3}H]thymidine incorporation (*A*) and the IFN-γ content was determined by ELISA (*B*). The values are presented as the mean ± SD for triplicate wells. The data are representative results of three independent experiments.

Local IL-23 secretion reduces CT26 tumorigenicity and metastatic ability

To analyze the effect of IL-23 on tumor growth, CT26 cells were infected with retroviral supernatant generated by transfecting pLNCX/scIL-23 into packaging cells. The G418-resistant CT26 bulk culture was established and designated as CT26/scIL-23. G418-resistant CT26 cells generated by infection with retroviral supernatants produced by pLNCX2 or pLNCX/scIL-12 were designated as CT26/LNCX and CT26/scIL-12, respectively, and were used as controls. The amount of scIL-12 released by CT26/scIL-12 cells was determined by a sandwich ELISA for murine IL-12 p70. In 72 h of culture, 2×10^5 CT26/scIL-12 cells produced 730 ± 47 ng/ml of murine IL-12. Because no ELISA system was available for IL-23, the relative amounts of IL-23 and IL-12 in CT26/scIL-23 and CT26/scIL-12 cell supernatants were determined by dot blot analysis using Ab against the common p40 subunit of the two cytokines. CT26/scIL-12 cells produced roughly fourfold more protein than did CT26/scIL-23 cells (data not shown). The biological activity of scIL-12 and scIL-23 produced by the transduced tumor cells was confirmed by the T cell proliferation assay as described above (data not shown).

IL-12 transduction has been shown to delay or completely abolish the in vivo growth of CT26 tumors (16). To evaluate the antitumor response induced by local secretion of IL-23, groups of 10 BALB/c mice were implanted s.c. with 1×10^5 live CT26/scIL-23 cells and were monitored for tumor development and survival. Mice receiving CT26/scIL-12 served as positive controls, and those injected with CT26/LNCX or wild-type CT26 cells were negative controls. CT26/scIL-23 cells and the control CT26/LNCX and CT26 cells initially showed the same tumor take, and all mice in these groups developed tumors by day 13 (Fig. 3*A*). The tumors in the CT26 and CT26/LNCX groups grew progressively, and by day 48 all animals either died or had been euthanized because the tumor size had reached the allowed limit. scIL-23-transduced CT26 cells showed a slightly slower growth rate than did the control tumors, but all CT26/scIL-23 tumors continued growing until day 26, when the mean tumor volume reached 521 ± 333 mm^3. Interestingly, after this initial growth, most tumors in the CT26/scIL-23 group started to regress, and 70% of the mice displayed complete tumor rejection by day 61 (Fig. 3*B*). In comparison, implantation of CT26/scIL-12 cells produced only palpable tumors in 80% of animals, and all of these tumors were quickly rejected by day 18 (Fig. 3).

To evaluate the antimetastatic effect of IL-23, groups of BALB/c mice ($n = 5$) were given CT26/LNCX, CT26/scIL-12, or CT26/scIL-23 cells by tail vein injection, and the number of pulmonary metastases in the different groups was counted on day 21 after injection. All animals receiving CT26/LNCX presented a large number (range 258–390) of metastatic foci in their lungs (Fig. 4*A*). Transduction of scIL-23 significantly reduced metastasis, with the number of lung foci ranging from zero to six ($p < 0.000001$ vs CT26/LNCX group). All mice injected with CT26/scIL-12 showed a complete absence of metastatic lung foci ($p < 0.000001$ vs CT26/LNCX group). We used an additional murine tumor model, B16F1 melanoma, to further evaluate the antimetastatic effect of IL-23. B16F1 cells secreting IL-23 (B16F1/scIL-23) were similarly produced by infection of B16F1 cells with scIL-23 retroviral supernatant and were selected in G418. B16F1/LNCX cells, generated by infection with retroviral supernatant produced by pLNCX2, were used as negative controls. C57BL/6 mice ($n =$

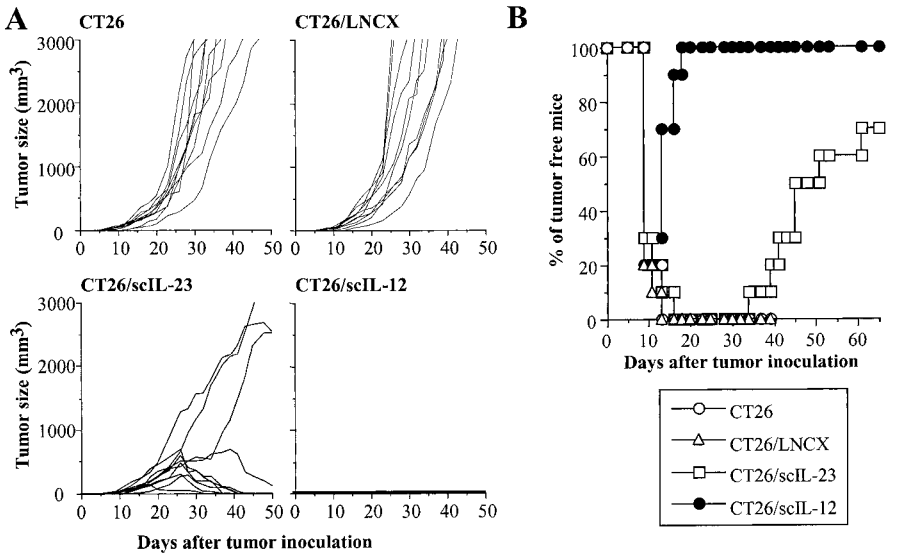

FIGURE 3. Tumor growth in, and survival of, BALB/c mice after s.c. implantation of tumor cells. BALB/c mice ($n = 10$) were injected s.c. with 1×10^5 transduced or nontransduced CT26 cells on day 0. *A*, Tumor volume of individual mice. *B*, Percentage of tumor-free animals in each group. The data are representative results for two independent experiments.

6) were inoculated with B16F1/scIL-23 or B16F1/LNCX by tail vein injection and were analyzed for lung metastasis. As shown in Fig. 4*B*, local expression of IL-23 significantly reduced the number of lung foci (range 1–11) compared with that of the control B16F1/LNCX cells (range 221–520; $p < 0.00001$). These results demonstrate that IL-23 was effective against metastatic tumors of different organ origins.

Induction of antitumor immune memory by CT26/scIL-23

To investigate whether a memory response developed in those animals that survived s.c. challenge with CT26/scIL-12 or CT26/scIL-23 cells, the tumor-free mice were subjected to s.c. rechallenge with parental CT26 cells. As shown in Fig. 5*A*, all animals in the CT26/scIL-12 and CT26/scIL-23 groups that had rejected tumors were resistant to CT26 challenge. In contrast, age-matched naive mice were uniformly susceptible to CT26 challenge. We also determined whether CTLs were present in animals that had rejected CT26/scIL-23 tumors. As shown in Fig. 5*B*, splenocytes from mice that had previously rejected CT26/scIL-23 tumors showed significant lytic activity against CT26 cells. The cytolytic activity induced by CT26/scIL-23 appeared to be tumor specific, because the splenocytes did not

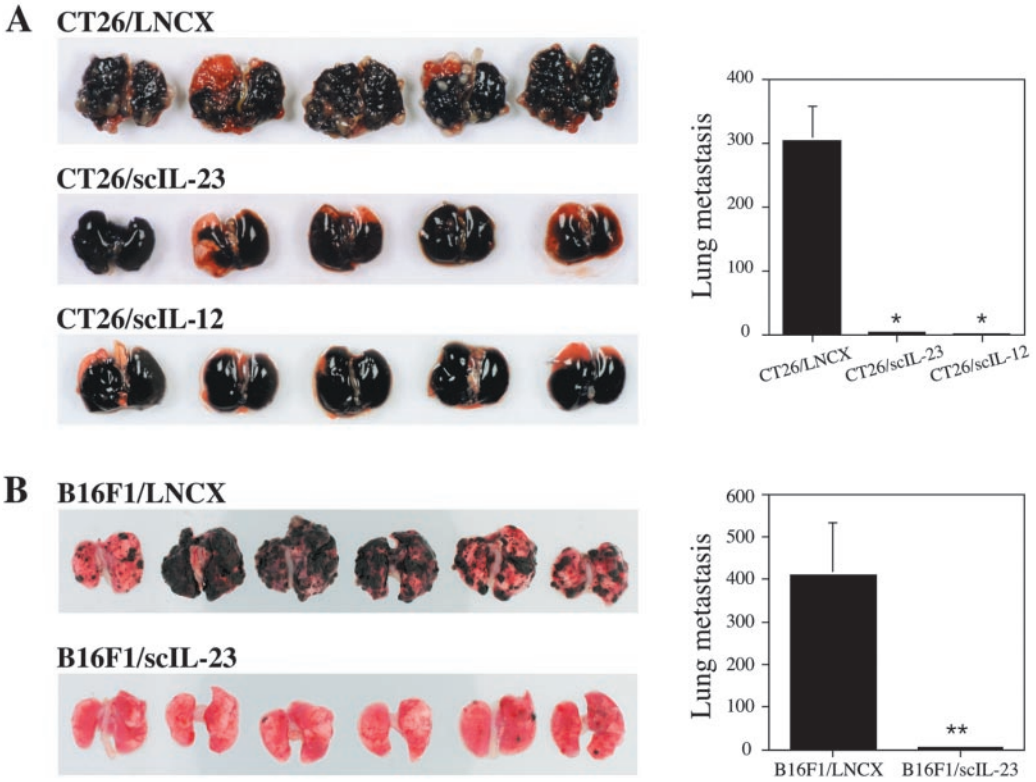

FIGURE 4. Lung metastases after i.v. injection of tumor cells. BALB/c ($n = 5$) (*A*) and C57BL/6 ($n = 6$) (*B*) mice were injected i.v. with 2×10^5 of the indicated tumor cells. The animals were killed on day 21 and tumor nodules in the lungs were counted. Data are presented as mean ± SD (*right*). Photographs of the lung of each group are also shown (*left*). The experiment was repeated twice with similar results. *, $p < 0.000001$, compared with the control CT26/LNCX group; **, $p < 0.00001$, compared with the control B16F1/LNCX group.

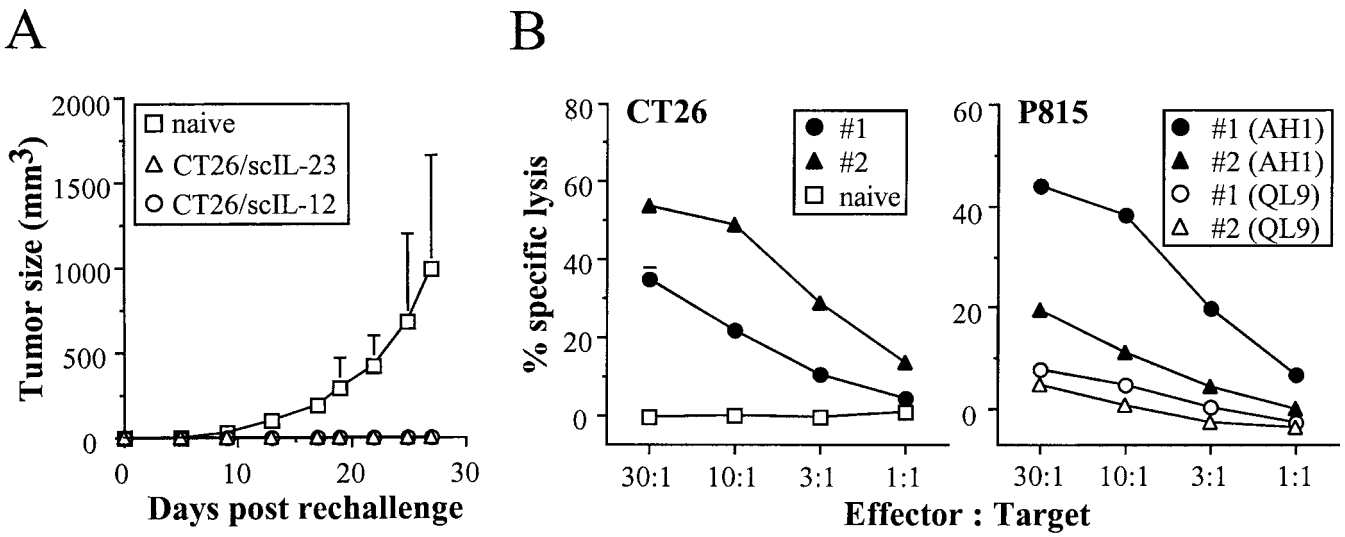

FIGURE 5. Induction of antitumor immunity after rejection of IL-23-transduced tumor cells. *A*, Animals that had previously rejected s.c. injected CT26/scIL-12 ($n = 10$) or CT26/scIL23 cells ($n = 6$) or age-matched naive controls ($n = 10$) were rechallenged s.c. with 1×10^5 parental CT26 cells, and the mean tumor volume in each group was monitored. *B*, CTL activity induced by CT26/scIL-23 cells. Splenocytes were collected from two animals (#1 and #2) that had previously rejected CT26/scIL23 cells or from an age-matched naive mouse, and they were restimulated in vitro for 5 days with CT26 cells. The specific cytolytic activity of the stimulated splenocytes was then tested on ^{51}Cr-labeled CT26 cells (*left panel*) and on ^{51}Cr-labeled P815 cells pulsed with 40 μg/ml peptide AH1 or QL9 (*right panel*). The values are presented as the mean ± SD of triplicate cultures. The CTL assays were repeated twice with similar results.

lyse P815 cells (data not shown). CT26 cells express an H-2L^d-restricted rejection epitope (AH1) derived from an endogenous retroviral gene product (13). AH1-specific cytolytic activity was induced in mice that had rejected CT26/scIL-23 cells, because splenocytes from these animals lysed P815 cells pulsed with AH1 peptide, but not with an irrelevant H-2L^d-binding peptide, QL9 (Fig. 5*B*).

Antitumor mechanisms of IL-23

We then analyzed the underlying cellular mechanisms contributing to the antitumor effect of IL-23. In the first series of experiments, immune-deficient SCID mice (deficient in B and T cells) and SCID/beige mice (deficient in B cells, T cells, and NK cells; $n = 5$–6) were injected s.c. with CT26/scIL-23 or CT26/LNCX cells, and the number of survivors was monitored. No antitumor activity of IL-23 was seen in either group, with all animals receiving CT26/scIL-23 cells developing tumors and dying by day 55 (Fig. 6). Compared with CT26/LNCX, CT26/scIL-23 cells showed the same tumor growth rate (data not shown) and resulted in the same mean survival time in these immune-deficient mice (42 ± 7 days vs 43 ± 4 days for the control group in SCID mice, $p > 0.05$; and 44 ± 8 days vs 44 ± 2 days for the control group in SCID/beige mice, $p > 0.05$). To further assess the role of CD4$^+$ and CD8$^+$ T cells and NK cells in the IL-23-mediated antitumor activity, BALB/c mice ($n = 5$) were depleted of these groups of cells by injection of anti-CD4 or anti-CD8 mAb or anti-asialo GM1 antiserum before and after CT26/scIL-23 inoculation. Mice treated with an irrelevant rat monoclonal IgG or normal rabbit serum at the same dose and schedule were included as controls. Flow cytometry showed that the treatments used depleted the appropriate cell population by 95% (data not shown). Depletion of CD8$^+$ T cells, but not of CD4$^+$ T cells, impaired the ability of naive mice to reject CT26/scIL-23 tumors. By day 48, the mean tumor volume in the CD8$^+$ T cell-depleted group was 2026 ± 690 mm^3, compared with 267 ± 287 mm^3 in the CD4$^+$ T cell-depleted group and 769 ± 570 mm^3 in the control IgG-treated group (Fig. 7*A*). In addition, all animals in the CD8$^+$ T cell-depleted group succumbed to CT26/scIL-23 tumor challenge, with a mean survival time of 56 ± 6 days, whereas 80% of mice in the CD4$^+$ T cell-depleted group and 60% in the control IgG-treated group were free of CT26/scIL-23 tumors and survived for the whole observation period of 120 days (data not shown). Depletion of NK cells had no effect on the antitumor activity of IL-23; CT26/scIL-23 cells

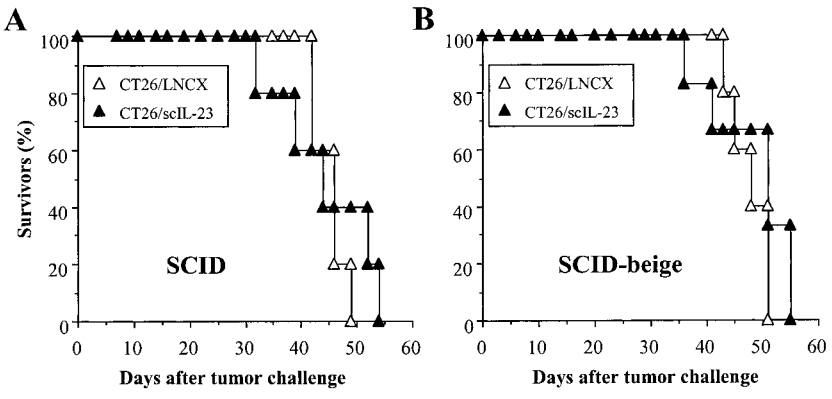

FIGURE 6. Survival of immunodeficient mice after s.c. implantation of tumor cells. SCID (*A*) or SCID/beige mice (*B*) ($n = 5$–6) were injected s.c. with 1×10^5 CT26/scIL-23 or CT26/LNCX cells on day 0, and the percentage of survivors in each group was monitored.

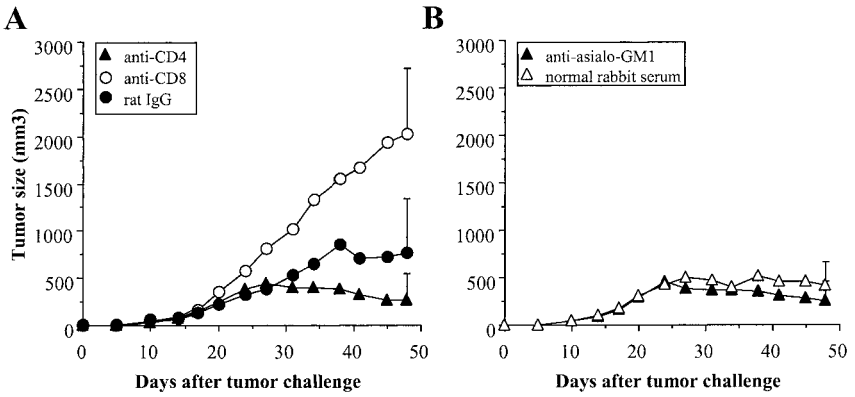

FIGURE 7. Effect of selective depletion of different lymphocyte populations on s.c. tumor growth in BALB/c mice. BALB/c mice ($n = 5$) were injected s.c. with 1×10^5 CT26/scIL-23 cells on day 0. *A*, Anti-CD4 or anti-CD8 mAb or a monoclonal normal rat IgG was injected i.p. on days −2, 0, 3, 5, 12, 19, 26, 33, 40, and 47 at a dose of 0.5 mg on day −2 and 0.25 mg subsequently. *B*, NK cells were depleted by i.p. injection of 20 μl of rabbit anti-asialo GM1 antiserum using the same schedule as above. Mice injected i.p. with normal rabbit serum were included as controls. The mean tumor volume in each group was monitored. The SD (bar) is only given for day 48 for clarity.

showed the same tumor growth rate in mice treated with anti-asialo GM1 antiserum or control rabbit serum (Fig. 7*B*), and the percentage of long-term survivors was the same (60%) in both groups.

We have also examined the phenotype of antitumor effector cells by immunohistochemical analysis of tumor tissue resected at various time points after injection of BALB/c mice with CT26/scIL-23. No $CD4^+$ or $CD8^+$ T cell infiltration was seen on days 12 (Fig. 8, *A* and *E*) and 20 (Fig. 8, *B* and *F*) after tumor injection, at which time the tumor cells were still growing progressively. On day 31, when tumors began to regress, moderate numbers of $CD4^+$ (Fig. 8*C*) and $CD8^+$ (Fig. 8*G*) T cells were present in the tumor tissues. On day 47, when tumors were in the later phase of regression, the number of infiltrating $CD8^+$ T cells was dramatically increased (Fig. 8*H*) and the number of $CD4^+$ T cells was slightly increased (Fig. 8*D*). Taken together, these data suggest that the predominant antitumor effector cells in the IL-23-mediated antitumor activity are $CD8^+$ T cells.

Discussion

In animal tumor models, IL-12 treatment has been reported to have potent antitumor activity against transplantable tumors, causing regression of established tumors and inhibiting tumor induction by chemical carcinogens and spontaneous arising of tumors in genetically modified mice (17). Unfortunately, the use of IL-12 in the clinic is limited by its considerable toxicity (18). The recently discovered cytokine IL-23 has a heterodimeric structure similar to that of IL-12, but it has a different immune cell-stimulating profile, raising the hope that it might be more useful in cancer treatment. In the present report, using IL-23-transduced tumor cells, we showed for the first time that IL-23 was very effective in inhibiting the growth of s.c. injected tumors and lung metastases. In addition, IL-23-secreting tumor cells elicited a strong CTL memory response against subsequent wild-type tumor challenge.

To investigate the antitumor effect of IL-23, we produced a retroviral vector encoding an scIL-23 fusion protein in the p40-p19 orientation connected by a flexible 18-aa peptide linker (Fig. 1*A*). Using the same peptide linker, a previously described scIL-12 fusion protein showed comparable biological activity to that of the native heterodimeric IL-12 (10). scIL-23 stimulated the proliferation of $CD4^+$ T cells as effectively as did scIL-12 (Fig. 2*A*), but in contrast to scIL-12, it did not induce IFN-γ production by $CD4^+$ T cells (Fig. 2*B*). In the mouse, IL-12 and IL-23 preferentially stimulate, respectively, the proliferation of naive ($CD4^+CD45Rb^{high}$) and memory ($CD4^+CD45Rb^{low}$) T cells (1). The $CD4^+$ T cells used in this study were shown by FACS analysis to contain both $CD45Rb^{high}$ and $CD45Rb^{low}$ cells (data not shown), and thus they could respond to both IL-12 and IL-23. Human IL-23 causes a moderate increase in IFN-γ production in human phytohemagglutinin blasts and activated memory T cells (CD45RO), but the level is significantly less than that induced by IL-12 treatment (1). The failure of scIL-23 to stimulate IFN-γ production in our study may be due to the presence of only a few memory cells in the $CD4^+$ T cell population, which was purified from naive wild-type mice, and/or the weak ability of IL-23 to stimulate IFN-γ production.

In this study, we showed that IL-23 had potent antitumor and antimetastatic activity in the murine CT26 carcinoma and B16F1 melanoma models. Most animals (70%, 7 of 10 mice) completely rejected scIL-23-transduced tumors and remained tumor free for the entire 120-day observation period (Fig. 3). This antitumor activity of IL-23 is remarkable when compared with that of IL-2 or GM-CSF, because transduction of these two cytokines into CT26 tumor cells results in few or no long-term tumor-free animals (19). In fact, we found that the antitumor activity of IL-23 was almost as great as that of IL-12, which is considered to be one of the most potent antitumor cytokines. However, the antitumor responses mediated by IL-12 and IL-23 were apparently different, the most striking difference being that IL-23-mediated tumor suppression was only evident at later time points after tumor injection. Whereas CT26/scIL-12 cells produced palpable tumors that were quickly rejected, all CT26/scIL-23 tumors grew progressively to a much larger size, and then regression was seen over a 2- to 3-wk period in most animals (Fig. 3*A*). The lack of an early response against scIL-23-transduced tumors was not due to differences in the intrinsic growth rate of CT26/scIL-23 cells, which have a similar in vitro doubling time to that of CT26/scIL-12 cells (data not shown). CT26/scIL-23 cells produced approximately fourfold less cytokine than did CT26/scIL-12 cells. However, differences in the cytokine production levels of the IL-23- and IL-12-secreting tumor cells cannot explain their distinctive antitumor responses, because we observed similar in vivo growth patterns with several cloned scIL-23-transduced CT26 tumor cells that secrete comparable amounts of cytokines to those produced by CT26/scIL-12 cells (data not shown).

The antitumor mechanisms of IL-12 have been extensively studied and involve both innate and adaptive immunity. The effector cells stimulated by IL-12 treatment include $CD8^+$ T cells, NK cells, and NKT cells (17). IFN-γ, which is mainly produced by T cells and NK cells, plays a major role in the antitumor activity of IL-12 (4, 20, 21). IFN-γ mediates tumor regression by stimulation of macrophages, upregulation of the expression of MHC proteins on tumor cells, and induction of the chemokine IFN-inducible protein 10, with consequent inhibition of angiogenesis (22). The lack of an early antitumor response in the presence of IL-23, seen in our study, may be due to its intrinsic lower ability to stimulate IFN-γ production, as shown in this study (Fig. 1*C*) and by Oppmann et al. (1). A recent study also showed that IL-23 overexpression in transgenic mice does not always

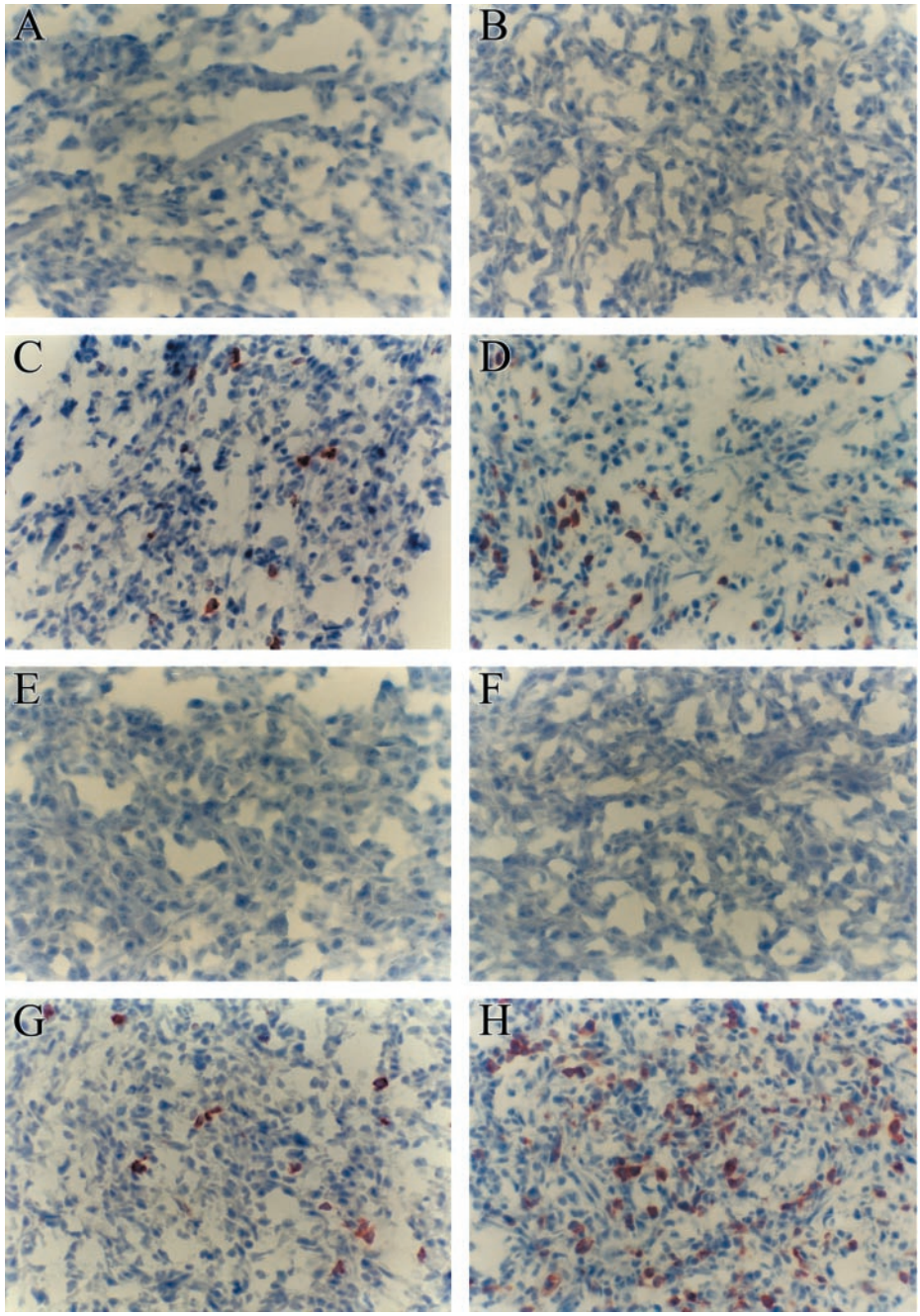

FIGURE 8. Immunohistochemical evaluation of CT26/scIL-23 tumor tissues. CT26/scIL-23 tumors at days 12 (*A* and *E*), 20 (*B* and *F*), 31 (*C* and *G*), and 47 (*D* and *H*) were stained with anti-CD4 (*A–D*) or anti-CD8 (*E–H*) mAbs. Sections were then incubated with streptavidin peroxidase and counterstained with hematoxylin.

result in increased in vivo IFN-γ production (23). In line with these findings, our unpublished data showed that the antitumor activity of IL-23 was not affected in mice depleted of IFN-γ. In regard to the cellular antitumor mechanisms of IL-23, our experiments in immunocompromised hosts and in animals selectively depleted of various lymphocyte populations strongly suggest that $CD8^+$ T cells play a crucial role in IL-23-mediated antitumor activity, because the protective effect was completely lost in T cell-deficient SCID mice (Fig. 6) and in wild-type mice depleted of $CD8^+$ T cells (Fig. 7*A*). Immunohistochemical analysis confirmed infiltration by $CD8^+$ T cells when tumor started to regress (Fig. 8*G*, day 31), and the number of infiltrating $CD8^+$ T cells was further increased at the later phase of tumor regression (Fig. 8*H*, day 47). We also observed moderate infiltration by $CD4^+$ T cells (Fig. 8, *C* and *D*), but these cells were apparently not required for the antitumor activity of IL-23 (Fig. 7*A*). In fact, we consistently observed a slower tumor growth rate of CT26/scIL-23 cells in $CD4^+$ T cell-depleted mice than in control mice, indicating that $CD4^+$ T cells might inhibit the IL-23-induced antitumor activity. A similar inhibitory effect of $CD4^+$ T cells on infiltration of $CD8^+$ T cells and NK cells into the tumor has been reported in mice challenged with IL-12-transduced CT26 cells (24). Because of technical difficulties, we have been unable to study NK cell infiltration in the CT26/scIL-23 tumors. However, the fact that NK cell depletion did not affect either the growth rate of CT26/scIL-23 cells (Fig. 7*B*) or the percentage of tumor-free animals strongly suggests that NK cells are not required for the antitumor activity of IL-23 in this CT26 tumor model.

Immunization of irradiated CT26 cells was known to induce low or nonprotective immunity (25, 26). In contrast, our results showed that local secretion of IL-23 resulted in strong antitumor immune memory against subsequent wild-type tumor challenge (Fig. 5*A*). A CT26 tumor-specific CTL response was induced in mice that

had rejected scIL-23-transduced tumors (Fig. 5*B*). This enhancement of the immune response by CT26/scIL-23 may be due to the effect of IL-23 on APCs, including dendritic cells and macrophages. Recent reports have shown that IFN-γ induces mouse bone marrow-derived macrophages to express the IL-23R (2) and that IL-23 can activate macrophages to produce proinflammatory cytokines (27). IL-23 also acts directly on dendritic cells to promote tumor peptide presentation to T cells (28). Furthermore, T cell responses may be amplified by the potent effect of IL-23 on memory-activated T cells (1). Together, these results suggest that IL-23-transduced tumors may function as an effective cancer vaccine for activating cellular immune responses. This is currently under investigation in our laboratory.

In summary, in this study, we show that IL-23, like IL-12, possesses potent antitumor and antimetastatic activity, but that it acts through a unique antitumor mechanism. The clinical use of IL-12 for cancer treatment is hampered by its associated toxic side effects (18), mostly due to the induction of high levels of IFN-γ. The unique action of IL-23, which results in less IFN-γ production, and its ability to activate APCs may provide an alternative and safer therapy for malignant diseases.

References

1. Oppmann, B., R. Lesley, B. Blom, J. C. Timans, Y. Xu, B. Hunte, F. Vega, N. Yu, J. Wang, K. Singh, et al. 2000. Novel p19 protein engages IL-12p40 to form a cytokine, IL-23, with biological activities similar as well as distinct from IL-12. *Immunity 13:715.*
2. Parham, C., M. Chirica, J. Timans, E. Vaisberg, M. Travis, J. Cheung, S. Pflanz, R. Zhang, K. P. Singh, F. Vega, et al. 2002. A receptor for the heterodimeric cytokine IL-23 is composed of IL-12Rβ1 and a novel cytokine receptor subunit, IL-23R. *J. Immunol. 168:5699.*
3. Brunda, M. J., L. Luistro, R. R. Warrier, R. B. Wright, B. R. Hubbard, M. Murphy, S. F. Wolf, and M. K. Gately. 1993. Antitumor and antimetastatic activity of interleukin 12 against murine tumors. *J. Exp. Med. 178:1223.*
4. Nastala, C. L., H. D. Edington, T. G. McKinney, H. Tahara, M. A. Nalesnik, M. J. Brunda, M. K. Gately, S. F. Wolf, R. D. Schreiber, W. J. Storkus, et al. 1994. Recombinant IL-12 administration induces tumor regression in association with IFN-γ production. *J. Immunol. 153:1697.*
5. Zou, J. P., N. Yamamoto, T. Fujii, H. Takenaka, M. Kobayashi, S. H. Herrmann, S. F. Wolf, H. Fujiwara, and T. Hamaoka. 1995. Systemic administration of rIL-12 induces complete tumor regression and protective immunity: response is correlated with a striking reversal of suppressed IFN-γ production by anti-tumor T cells. *Int. Immunol. 7:1135.*
6. Boggio, K., G. Nicoletti, E. Di Carlo, F. Cavallo, L. Landuzzi, C. Melani, M. Giovarelli, I. Rossi, P. Nanni, C. De Giovanni, et al. 1998. Interleukin 12-mediated prevention of spontaneous mammary adenocarcinomas in two lines of Her-2/neu transgenic mice. *J. Exp. Med. 188:589.*
7. Roy, E. J., U. Gawlick, B. A. Orr, L. A. Rund, A. G. Webb, and D. M. Kranz. 2000. IL-12 treatment of endogenously arising murine brain tumors. *J. Immunol. 165:7293.*
8. Corbett, T. H., D. P. J. Griswold, B. J. Roberts, J. C. Peckham, and F. M. J. Schabel. 1975. Tumor induction relationships in development of transplantable cancers of the colon in mice for chemotherapy assays, with a note on carcinogen structure. *Cancer Res. 35:2434.*
9. Talmadge, J. E., and I. J. Fidler. 1982. Cancer metastasis is selective or random depending on the parent tumor population. *Nature 297:593.*
10. Lee, Y. L., Y. L. Ye, C. I. Yu, Y. L. Wu, Y. L. Lai, P. H. Ku, R. L. Hong, and B. L. Chiang. 2001. Construction of single-chain interleukin-12 DNA plasmid to treat airway hyperresponsiveness in an animal model of asthma. *Hum. Gene Ther. 12:2065.*
11. Chow, Y. H., B. L. Chiang, Y. L. Lee, W. K. Chi, W. C. Lin, Y. T. Chen, and M. H. Tao. 1998. Development of Th1 and Th2 populations and the nature of immune responses to hepatitis B virus DNA vaccines can be modulated by codelivery of various cytokine genes. *J. Immunol. 160:1320.*
12. Huang, T. H., P. Y. Wu, C. N. Lee, H. I. Huang, S. L. Hsieh, J. Kung, and M. H. Tao. 2000. Enhanced antitumor immunity by fusion of CTLA-4 to a self tumor antigen. *Blood 96:3663.*
13. Huang, A. Y., P. H. Gulden, A. S. Woods, M. C. Thomas, C. D. Tong, W. Wang, V. H. Engelhard, G. Pasternack, R. Cotter, D. Hunt, et al. 1996. The immunodominant major histocompatibility complex class I-restricted antigen of a murine colon tumor derives from an endogenous retroviral gene product. *Proc. Natl. Acad. Sci. USA 93:9730.*
14. Sykulev, Y., A. Brunmark, T. J. Tsomides, S. Kageyama, M. Jackson, P. A. Peterson, and H. N. Eisen. 1994. High-affinity reactions between antigen-specific T-cell receptors and peptides associated with allogeneic and syngeneic major histocompatibility complex class I proteins. *Proc. Natl. Acad. Sci. USA 91:11487.*
15. Wilkinson, V. L., R. R. Warrier, T. P. Truitt, P. Nunes, M. K. Gately, and D. H. Presky. 1996. Characterization of anti-mouse IL-12 monoclonal antibodies and measurement of mouse IL-12 by ELISA. *J. Immunol. Methods 189:15.*
16. Colombo, M. P., M. Vagliani, F. Spreafioo, M. Parenza, C. Chiodoni, C. Melani, and A. Stoppacciaro. 1996. Amount of interleukin 12 available at the tumor site is critical for tumor regression. *Cancer Res. 56:2531.*
17. Colombo, M. P., and G. Trinchieri. 2002. Interleukin-12 in anti-tumor immunity and immunotherapy. *Cytokine Growth Factor Rev. 13:155.*
18. Leonard, J. P., M. L. Sherman, G. L. Fisher, L. J. Buchanan, G. Larsen, M. B. Atkins, J. A. Sosman, J. P. Dutcher, N. J. Vogelzang, and J. L. Ryan. 1997. Effects of single-dose interleukin-12 exposure on interleukin-12-associated toxicity and interferon-γ production. *Blood 90:2541.*
19. Vagliani, M., M. Rodolfo, F. Cavallo, M. Parenza, C. Melani, G. Parmiani, G. Forni, and M. P. Colombo. 1996. Interleukin 12 potentiates the curative effect of a vaccine based on interleukin 2-transduced tumor cells. *Cancer Res. 56:467.*
20. Tsung, K., J. B. Meko, Y. L. Tsung, G. R. Peplinski, and J. A. Norton. 1998. Immune response against large tumors eradicated by treatment with cyclophosphamide and IL-12. *J. Immunol. 160:1369.*
21. Segal, J. G., N. C. Lee, Y. L. Tsung, J. A. Norton, and K. Tsung. 2002. The role of IFN-γ in rejection of established tumors by IL-12: source of production and target. *Cancer Res. 62:4696.*
22. Coughlin, C. M., K. E. Salhany, M. S. Gee, D. C. LaTemple, S. Kotenko, X. Ma, G. Gri, M. Wysocka, J. E. Kim, L. Liu, et al. 1998. Tumor cell responses to IFNγ affect tumorigenicity and response to IL-12 therapy and antiangiogenesis. *Immunity 9:25.*
23. Wiekowski, M. T., M. W. Leach, E. W. Evans, L. Sullivan, S. C. Chen, G. Vassileva, J. F. Bazan, D. M. Gorman, R. A. Kastelein, S. Narula, and S. A. Lira. 2001. Ubiquitous transgenic expression of the IL-23 subunit p19 induces multiorgan inflammation, runting, infertility, and premature death. *J. Immunol. 166:7563.*
24. Martinotti, A., A. Stoppacciaro, M. Vagliani, C. Melani, F. Spreafico, M. Wysocka, G. Parmiani, G. Trinchieri, and M. P. Colombo. 1995. CD4 T cells inhibit in vivo the CD8-mediated immune response against murine colon carcinoma cells transduced with interleukin-12 genes. *Eur. J. Immunol. 25:137.*
25. Fakhrai, H., D. L. Shawler, R. Gjerset, R. K. Naviaux, J. Koziol, I. Royston, and R. E. Sobol. 1995. Cytokine gene therapy with interleukin-2-transduced fibroblasts: effects of IL-2 dose on anti-tumor immunity. *Hum. Gene Ther. 6:591.*
26. Wang, X. Y., Y. Li, M. H. Manjili, E. A. Repasky, D. M. Pardoll, and J. R. Subjeck. 2002. Hsp110 over-expression increases the immunogenicity of the murine CT26 colon tumor. *Cancer Immunol. Immunother. 51:311.*
27. Cua, D. J., J. Sherlock, Y. Chen, C. A. Murphy, B. Joyce, B. Seymour, L. Lucian, W. To, S. Kwan, T. Churakova, et al. 2003. Interleukin-23 rather than interleukin-12 is the critical cytokine for autoimmune inflammation of the brain. *Nature 421:744.*
28. Belladonna, M. L., J. C. Renauld, R. Bianchi, C. Vacca, F. Fallarino, C. Orabona, M. C. Fioretti, U. Grohmann, and P. Puccetti. 2002. IL-23 and IL-12 have overlapping, but distinct, effects on murine dendritic cells. *J. Immunol. 168:5448.*